SAND77-0376
Unlimited Release

Circular Microstrip Antennas

George H. Schnetzer

Prepared by Sandia Laboratories, Albuquerque, New Mexico 87115
and Livermore, California 94550 for the United States Energy Research
and Development Administration under Contract AT(29–1)-789

Printed April 1977

Sandia Laboratories

SF 2900 Q(7-73)

DISCLAIMER

Issued by Sandia Laboratories, operated for the United States Energy Research & Development Administration by Sandia Corporation.

Printed in the United States of America
Available from:
National Technical Information Service
U.S. Department of Commerce
5285 Port Royal Road
Springfield, VA 22161
Price: Printed Copy $4.00; Microfiche $3.00

SAND 77-0376
UNLIMITED RELEASE

CIRCULAR MICROSTRIP ANTENNAS

GEORGE H. SCHNETZER
ANTENNA DEVELOPMENT DIVISION 2123
SANDIA LABORATORIES
ALBUQUERQUE, NEW MEXICO 87115

PRINTED APRIL 1977

ABSTRACT (U)

The circular microstrip antenna is analyzed by developing the field equations within the antenna in terms of Bessel functions. When the order of the Bessel functions is 1, the antenna radiates normal to the surface on which the antenna is mounted. Equations are developed for calculation of radiation patterns, impedance, bandwidth and efficiency when the antenna is operating in this mode. Curves are provided to assist in the design of a circular microstrip antenna.

Table of Contents

List of Figures

CIRCULAR MICROSTRIP ANTENNAS

INTRODUCTION

Microstrip antennas have been used extensively in applications where the antenna must have a very low profile. Some characteristics of rectangular microstrip antennas have been covered in previous reports.[1,2] In this report the circular microstrip, shown in Figure 1, is analyzed and its characteristics presented in the form of simple equations and graphs. The antenna is an annular section of copper clad dielectric material with the two copper surfaces shorted together around the inner radius, r_i. This antenna is not as easily fabricated as the rectangular microstrip antenna but offers one significant advantage. The outer radius, r_o, is not fixed by the frequency and dielectric constant of the substrate so the outer radius can be selected to obtain the best pattern. Once r_o is determined, the inner radius can be determined to obtain the desired resonant frequency.

MODES OF OPERATION

In cylindrical structures the fields can be conveniently expressed in terms of Bessel functions of order ν. Since the antenna is very thin, relative to a wavelength, no variation in the z direction of the fields will be assumed and consequently E_r and E_ϕ are both zero in the annular region between the plate. (See Figure 2).

$$E_z = [AH_\nu^{(1)}(k_c r) + BH_\nu^{(2)}(k_c r)][C \cos \nu\phi + D \sin \nu\phi] \quad (1)$$

where

$$H_\nu^{(1)}(k_c r) = J_\nu(k_c r) + jY_\nu(k_c r)$$

$$H_\nu^{(2)}(k_c r) = J_\nu(k_c r) - jY_\nu(k_c r)$$

this form of the Bessel functions separates the fields into radially propagating waves; $H_\nu^{(1)}(k_c r)$ is a wave propagating in the -r direction and $H_\nu^{(2)}(k_c r)$ is a wave propagating in the +r direction. Also, due to symmetry, the coefficient of sin $\nu\phi$ must be zero.

$$E_z = \cos \nu\phi[A_1 H_\nu^{(1)}(k_c r) + B_1 H_\nu^{(2)}(k_c r)] \quad (2)$$

The other non-zero field components are

$$H_\phi = \frac{-j\omega\varepsilon}{k_c^2} \frac{\partial E_z}{\partial r} \quad (3)$$

$$H_r = \frac{j\omega\varepsilon}{r k_c^2} \frac{\partial E_z}{\partial \phi} \quad (4)$$

The radiation admittance of the cylindrical aperture formed by the two plates is much less than the admittance of the radial transmission lines. Therefore, for a first order approximation, to determine the resonant frequency, this aperture can be considered an open circuit so there is no current in the radial direction at the outer radius.

$$H_\phi \Big|_{r=r_o} = \frac{-j\omega}{k_c^2} \frac{\partial E_z}{\partial r} \Big|_{r=r_o} = 0 \quad . \tag{5}$$

Since the two plates are shorted together at the inner radius, the E field must be zero at that point.

$$\cos \nu\phi \left[A_1 H_\nu^{(1)}(k_c r_i) + B_1 H_\nu^{(2)}(k_c r_i) \right] = 0 \tag{6}$$

These two equations determine the resonant conditions, the k_c's which are a solution to equations 5 and 6, for any order of the Bessel functions. This k_c is equivalent to $2\pi/\lambda_c$ where λ_c is the cutoff wavelength cylindrical waveguide which propagates in the z direction. When such a waveguide is operated at cutoff, the guide wavelength approaches infinity and there is no variations in the z direction. In the perfect model which has been assumed for determining resonant frequencies, no power loss through the outer aperture, if there were no losses in the plates or dielectric, the fields in the annular region could have only discrete frequency values corresponding to the k_c's for that geometry. In the realistic case of some radiation from the edges and small losses in the plates, the fields will have significant amplitude in narrow bands around these resonant frequencies.

The order of the Bessel functions, ν, can have any integer value. When $\nu = 0$ the antenna is essentially identical to an annular slot which has a pattern similar to a monopole. This is not the order which is of primary interest in this report but

the resonant frequency will be determined for this order since it is the lowest resonant frequency. For $\nu = 0$ equation 5 becomes

$$\frac{j\omega\varepsilon}{k_c}\left[A_1 H_1^{(1)}(k_c r_o) + B_1 H_1^{(2)}(k_c r_o)\right] = 0 \tag{7}$$

and equation 6 is

$$\left[A_1 H_o^{(1)}(k_c r_i) + B_1 H_o^{(2)}(k_c r_i)\right] = 0 \tag{8}$$

These equations can be combined.

$$\frac{H_o^{(1)}(k_c r_i)}{H_o^{(2)}(k_c r_i)} = \frac{H_1^{(1)}(k_c r_o)}{H_1^{(2)}(k_c r_o)} \tag{9}$$

For any given r_i and r_o there are an infinite number of values of k_c which are solutions to equation 9. The lowest value is the solution desired and is analagous to the case of a one quarter wavelength line shorted at one end and open at the other. This solution is plotted in Figure 3. Both $k_c r_o$ and the ratio $k_c r_o / k_c r_i$ are plotted vs $k_c r_i$ for convenience. In an analysis of a fixed geometry, the ratio $r_o/r_i = k_c r_o / k_c r_i$ is known so the ratio curve can be used to determine the value $k_c r_i$ and consequently the resonant frequency. In a design effort, the desired resonant frequency and one of the radii is known so the $k_c r_o$ curve can be used to determine the other radius.

$$k_c = 2\pi/\lambda_d \tag{10}$$

where λ_d = wavelength in the dielectric material

This mode will be called the zero-order mode for this antenna type and operating in this mode would be a convenient way to obtain a low profile antenna with a pattern similar to a dipole.

The case of primary interest in this report is when $\nu = 1$, one cycle variation in the ϕ direction of the fields. The resonant frequencies are determined in a similar manner, equation 5 becomes

$$\frac{-j\omega\varepsilon \cos\phi}{k_c}\left\{A_1\left[k_c H_o^{(1)}(k_c r_o) - \frac{1}{r_o} H_1^{(1)}(k_c r_o)\right] + B_1\left[k_c H_o^{(2)}(k_c r_o) - \frac{1}{r_o} H_1^{(2)}(k_c r_o)\right]\right\} = 0 \tag{11}$$

and equation 6 is

$$\cos\phi\left[A_1 H_1^{(1)}(k_c r_i) + B_1 H_1^{(2)}(k_c r_i)\right] = 0 \tag{12}$$

These equations can be combined to yield

$$\frac{H_1^{(1)}(k_c r_i)}{H_1^{(2)}(k_c r_i)} = \frac{r_o k_c H_o^{(1)}(k_c r_o) - H_1^{(1)}(k_c r_o)}{r_o k_c H_o^{(2)}(k_c r_o) - H_1^{(2)}(k_c r_o)} \tag{13}$$

The lowest frequency solution to this equation is plotted in Figure 4. Again, both $k_c r_o$ and the ratio $k_c r_o / k_c r_i$ are plotted vs $k_c r_i$ for convenience.

By comparing Figures 3 and 4, there is very little difference between the resonant frequencies for the zero-order and 1st order modes for large radii. For very large radii, the two modes may exist simultaneously and either a different feeding or mode suppression techniques must be used to eliminate the undesirable mode. By driving the antenna at two points, $\phi = 0$ and π, out of phase, the 1st order mode will be excited but the zero order mode will not. Similarly, if the antenna is driven at the same two points but in phase, the zero-order mode will be excited and not the 1st order mode. Shorting pins placed in the E field nodes of the 1st order mode, $\phi = \pi/2$ and $3\pi/2$, will also kill the zero-order mode and have no effect on the 1st order mode.

PATTERNS

The radiation pattern of the circular microstrip which is mounted on a large ground plane can be easily calculated since the voltage distribution is known for a given value of ν. Since the microstrip antenna is very thin relative to a wave length, the voltage around the aperture can be replaced by an equivalent magnetic current filament as was done for the rectangular microstrip antenna.[1] This equivalent magnetic current filament for $\nu = 1$ is

$$\overline{I_m} = 2V_o \cos \phi' \, \hat{a}_\phi \tag{14}$$

where $\hat{a}_\phi = \sin \phi' \, \hat{a}_x + \cos \phi' \, \hat{a}_y$

The coordinate system for the pattern calculations is shown in Figure 5. The electric vector potential for this magnetic current distribution is

$$\overline{F} = \frac{\varepsilon e^{-jkr}}{4\pi r} \int \overline{I_m} \, e^{jkr'} = \frac{\varepsilon e^{-jkr}}{4\pi r} \overline{L} \tag{15}$$

where

$$r' = r_o(\cos \phi' \cos \phi + \sin \phi' \sin \phi)\sin \theta$$

$$d\ell = r_o \, d\phi'$$

The components of the radiated field can be obtained from the above integral, $\overline{L}$.

$$E_\theta = -j \frac{e^{-jkr}}{2\lambda r} L\phi \tag{16}$$

$$E_\phi = j \frac{e^{-jkr}}{2\lambda r} L\theta \tag{17}$$

$$L_\phi = L_x \sin \phi + L_y \cos \phi \tag{18}$$

$$L_\theta = L_x \cos \phi \cos \theta + L_y \sin \phi \cos \theta \tag{19}$$

The principle plane patterns, $\phi = 0$ and 90, have been calculated and are plotted in Figures 6-10 for $r_o/\lambda = .1, .2, .3, .4,$ and $.5$. Due to symmetry, in both the $\phi = 0$ and $\phi = 90$ planes, only half the patterns are plotted, the other half being a mirror image. Also, due to symmetry $E_\theta = 0$ when $\phi = 90^o$ or 270^o and $E_\theta = 0$ when $\phi = 0$ or 180^o. Increasing the radius decreases the beamwidths and increases the gain up to r_o/λ of .3. For radii greater than this, the beamwidths continue to decrease but another lobe forms at $\theta = 90$ degrees so the gain does not go up much more. The half power beamwidths are plotted in Figure 11.

IMPEDANCE, BANDWIDTH, AND EFFICIENCY

Developing the expressions for the fields between the conducting plates in terms of radially propagating waves leads directly to an equivalent circuit model for the antenna as shown in Figure 12. The admittance of the aperture is Y_a which is shunted by a shorted transmission line. This transmission line is a radial line where the characteristic admittance and the propagation constant are both a function of the radius as well as the order, ν, of the Bessel Functions. It is analagous to a one quarter wavelength uniform line shunting the aperture. The properties developed here will only be for the 1st order mode, $\nu = 1$.

Determining the total admittance of the radiating aperture is very difficult but the real part of this admittance can be obtained by integrating the total radiated power. The imaginary

part of the admittance will be canceled by the shunting transmission line so it is of little importance anyway. The real part of the admittance of the aperture, G_a, will be defined as

$$G_a' = \frac{P_{rad}}{|V|^2} \tag{20}$$

where

P_{rad} is the total radiated power

V is the RMS voltage between the plates at $r = r_o$ and $\phi = 0$.

This conductance has been calculated for values of r_o from .1 to 1. wavelength and is plotted in Figure 13. The sharp rise in the conductance for r_o/λ between .4 and .7 is due to the second lobe, at $\theta = 90$, becoming significant.

To determine the effect of the shunting transmission line the characteristic admittance must be known. Obviously, when the antenna is resonant the susceptance of this shunt line cancels the susceptance of the aperture and the input admittance will be just the aperture conductance G_a. For frequencies slightly away from resonance, the susceptance of this shunting line will determine the bandwidth of the antenna. Due to the thinness of the line, the characteristic admittance of the line will be very much greater than the aperture conductance.

To be consistant with the definition of aperture conductance the admittance of the radial line will be

$$Y_o(r) = \frac{P_{av}}{|V(r)|^2} \tag{21}$$

where P_{av} is the average power for a wave traveling in either radial direction and $V(r)$ is the voltage between the plates at $\phi = 0$.

Since the antenna is very thin

$$|V(r)| = T\left|E_z\right|_{\phi=0} . \tag{22}$$

The average power in an inward propagating wave is

$$P_{av} = \int_0^T \int_0^{2\pi} R_e[E_z H_\phi^*]dzrd\phi \tag{23}$$

$$= Tr \int_0^{2\pi} R_e[E_z H_\phi^*]d\phi$$

The fields for an inward traveling wave as

$$E_z = AH_1^{(1)}(k_c r) \cos \phi \tag{24}$$

$$H_\phi \frac{-j\omega\varepsilon A}{k_c}\left(H_o^{(1)}(k_c r) - \frac{1}{k_c r} H_1^{(1)}(k_c r)\right) \cos \phi \tag{25}$$

The radial component of the real part of the complex Poynting vector is

$$R_e[E_z H_\phi^*] = A^2 \cos^2 \phi \left(\frac{\omega\varepsilon}{k_c}\right)\left(J_1(k_c r)Y_o(k_c r) - Y_1(k_c r)J_o(k_c r)\right) \tag{26}$$

The average power is

$$P_{av} = A^2 Tr\left(\frac{\omega\varepsilon}{k_c}\right)\left(J_1(k_c r)Y_o(k_c r) - Y_1(k_c r)J_o(k_c r)\right) \int_0^{2\pi} \cos^2 \phi d\phi$$

$$= \pi A^2 Tr\left(\frac{\omega\varepsilon}{k_c}\right)\left(J_1(k_c r)Y_o(k_c r) - Y_1(k_c r)J_o(k_c r)\right) \tag{27}$$

The characteristic admittance is given by

$$Y_o(r) = \frac{\sqrt{\varepsilon_r}\, r}{120T} \frac{\left[J_1(k_c r)Y_o(k_c r) - Y_1(k_c r)J_o(k_c r)\right]}{\left|H_1^{(1)}(k_c r)\right|^2} \tag{28}$$

$$= \frac{\sqrt{\varepsilon_r}\, r}{120T} F(r)$$

The function, F(r), is plotted in Figure 14 vs $k_c r$.

At frequencies near the resonant frequency of the microstrip antenna the shorted transmission line provides a very low admittance shunting the aperture admittance. The electrical length of the line is approximately $\pi/2$ so for a first order approximation to determine the bandwidth this radial line will be replaced with a uniform line, $\lambda/4$ long, with a characteristic admittance of $Y_o(r_o)$. The shunt susceptance of this line is

$$Y_s = -jY_o(r_o) \cot \theta \tag{29}$$

The Q of a parallel resonant circuit can be determined from

$$Q = \frac{f_o}{\Delta f} \tag{30}$$

where f_o = resonant frequency

Δf = frequency between half-power points

The half power points are defined on the frequency where the magnitude of the shunt susceptance equals the shunt conductance. Rearranging equation 29 yields

$$Y_s = -jY_o(r_o)\frac{\cos\theta}{\sin\theta} = jY_o(r_o)\frac{\sin(\theta - \pi/2)}{\sin\theta} \tag{31}$$

Since $\theta \sim \pi/2$

$$Y_s \approx jY_o(r_o)\sin(\theta - \pi/2) \tag{32}$$

For small arguments sin x can be approximated by x

$$Y_s \approx jY_o(r_o)(\theta - \pi/2)$$

Since θ is a linear function of frequency in the simple approximate model

$$\theta = \frac{\pi}{2}\frac{f}{f_o} \tag{34}$$

The half power frequencies, where the shunt susceptance equals the aperture conductance, can be determined by

$$G_a = Y_o(r_o)\ \frac{\pi}{2}\left(\frac{f}{f_o} - 1\right) = Y_o(r)\frac{\pi}{2}\left(\frac{\Delta f}{2f_o}\right) \tag{35}$$

The Q is then

$$Q = \frac{f_o}{\Delta f} = \frac{Y_o(r_o)\pi}{4Ga} \tag{36}$$

The bandwidth, which can be obtained, can be determined from the Q and the amount of broadband matching used.[4] Without any broadband matching, the fractional bandwidth will just be 1/Q.

In the above analysis the radial transmission line was assumed lossless and in a realistic case, the power dissipated in the line will be very small relative to the energy stored in the line. But, the power lost in the line may not be small relative to the power being radiated by the aperture. When this loss is ignored, the calculated value of input admittance is lower and the calculated value of Q higher than the measured values. Therefore, to have a good model, the effect of these losses must be taken into account.

Since the power dissipated in the line is small relative to the energy stored, the fields in the line are not reduced significantly by this loss. Therefore, the fields within the line will be assumed to be the same as in the lossless case, the power dissipated in the conductors and dielectric will be calculated for these field levels, and the effect of this loss on the model will be accounted for by an additional shunt conductance across the aperture.

The power loss per unit area in a conducting surface is[5]

$$W_L = R_s |J_s|^2 \tag{37}$$

where J_s is the RMS surface current density

$R_s = \sqrt{\frac{\pi f \mu}{\sigma}}$ is the surface resistivity.

The surface current is just equal to the total H field at the conductor surface

$$|J_s|^2 = |H_\phi|^2 + |H_r|^2 \tag{38}$$

The total electric field in the standing waves are

$$E_z = \left[A H_1^{(1)}(k_c r) + B H_1^{(2)}(k_c r) \right] \cos \phi \tag{39}$$

Since the E field must be zero at r_i

$$\frac{B}{A} = \frac{-H_1^{(1)}(k_c r_i)}{H_1^{(2)}(k_c r_i)} \tag{40}$$

The two components of the H field are

$$H_\phi = \frac{-j\omega\varepsilon}{k_c r} \left\{ A \left(H_o^{(1)}(k_c r) - \frac{1}{k_c r} H_1^{(1)}(k_c r) \right) + B \left(H_o^{(2)}(k_c r) - \frac{1}{k_c r} H_1^{(2)}(k_c r) \right) \right\} \cos \phi \tag{41}$$

$$H_r = \frac{-j\omega\varepsilon}{k_c r} \left[A H_1^{(1)}(k_c r) + B H_1^{(2)}(k_c r) \right] \sin \phi \tag{42}$$

The total power dissipated in the 2 conductive surfaces is

$$W_c = 2R_s \int_0^{2\pi} \int_{r_i}^{r_o} |H_\phi|^2 + |H_r|^2 \, r dr d\phi$$

$$= \frac{1}{\sqrt{\sigma}} \frac{\varepsilon_r \sqrt{\pi f \varepsilon_o}}{60} \int_{r_i}^{r_o} |F_\phi|^2 + |F_r|^2 \, r dr$$

$$= \frac{1}{\sqrt{\sigma}} F_c(\varepsilon_r, r_o, f) \tag{43}$$

where

$$F_\phi = A\left(H_o^{(1)}(k_c r) - \frac{1}{k_c r} H_1^{(1)}(k_c r)\right) \tag{44}$$

$$+ B\left(H_o^{(2)}(k_c r) - \frac{1}{k_c r} H_1^{(2)}(k_c r)\right)$$

$$F_r = AH_1^{(1)}(k_c r) + BH_1^{(2)}(k_c r) \, . \tag{45}$$

The function F_c is a function only of ε_r, r_o and f, since r_i, the lower limit of integration, is determined by the other three variables for a resonant antenna.

The total power dissipated in the dielectric material is

$$W_d = \int_{vol} \omega \varepsilon'' \, |E|^2 \, dv \tag{46}$$

where $\varepsilon'' = \varepsilon_o \varepsilon_r \tan \delta$

$\tan \delta$ is the loss tangent.

The above integral becomes

$$W_d = \omega\varepsilon_o\varepsilon_r \tan\delta \int_0^T \int_0^{2\pi} \int_{r_i}^{r_o} |E_z|^2 \, r dr d\phi dz$$

$$= T\omega\varepsilon_o\varepsilon_r \tan\delta \int_0^{2\pi} \int_{r_i}^{r_o} |E_z|^2 \, r dr d\phi$$

$$= \tan\delta \; T \; \omega\pi\varepsilon_o\varepsilon_r \int_{r_i}^{r_o} |F_r|^2 \, r dr$$

$$= \tan\delta \; T \; F_d(\varepsilon_r, f, r_o) \tag{47}$$

Equivalent conductance to use in the model, Figure 15, is

$$G_s = \frac{W_c + W_d}{|V|^2} = G_{sc} + G_{sd} \tag{48}$$

The voltage at the outer edge

$$|V| = |E_z(r_o, o)|T \tag{49}$$

$$= |F_r(r_o)|T$$

The two conductances are then

$$G_{sc} = \frac{F_c}{\sqrt{\sigma}\, T^2 |F_r(r_o)|^2} \tag{50}$$

$$G_{sd} = \frac{\tan \delta \; F_d}{T|F_r(r_o)|^2} \tag{51}$$

The quantities $\frac{F_c}{|F_r(r_o)|^2}$ and $\frac{F_d}{|F_r(r_o)|^2}$ are plotted vs r_o in Figures 16-21 for ε_r = 2.5, 4. and 10. and frequencies of 500, 1000, 2000, and 4000 MHz.

With these curves, it should be possible to estimate reasonably well the loss conductances for most any frequency, conductor material and dielectric constant. Equations 50 and 51 show the strong effect the thickness has on the losses in a microstrip antenna. The efficiency of the antenna is easily determined from the model.

$$\text{Eff.} = \frac{G_a}{G_a + G_{sc} + G_{sd}} \tag{52}$$

Unless the loss conductances in the antenna are extremely large, the admittance of the antenna at the aperture will be much less than 20 mmhos necessary for a match to normal 50 ohm transmission lines. One way around this problem is to feed the antenna at a point where the radius is less than r_o. If the power delivered to the antenna remains the same as the feed point is moved toward the center, the real part of the input conductance must vary as $1/|V|^2$.

$$G_{in}(r) = \frac{G_{in}(r_o)}{|V(r_o)|^2} |V(r)|^2$$

$$= \frac{|F_r(r)|^2}{|F_r(r_o)|^2} G_{in}(r_o) \qquad (53)$$

The ratio $\frac{|F_r(r)|^2}{|F_r(r_o)|^2}$ is primarily dependent upon the distance from the inner radius, r_i, compared to the difference between r_o and r_i and is only slightly dependent upon the overall radius or $k_c r_o$. This ratio is plotted in Figure 22 vs $\frac{r - r_i}{r_o - r_i}$ for $k_c r_o$ of 1.85 and 4.0. Once the conductance at the aperture antenna is determined, both aperture conductance and loss conductances, Figure 22 can be used to determine the location which will produce an antenna with the desired input impedance at resonance.

CONCLUSIONS

The curves and equations developed in this report provide sufficient data to design a circular microstrip antenna without depending upon a lot of empirical effort. Due to the fringing capacitance at the outer end of the radial line and the unknown susceptance of the aperture, the exact value of the radii cannot be calculated. Using the radii determined from Figure 4 will provide an antenna with a resonant frequency which is just slightly

less than desired. This can be compensated for by trimming the outer radius slightly to increase the resonant frequency. The curves for determining input conductance, Q and efficiency have been found to provide good agreement with measured data.

REFERENCES

1. G. H. Schnetzer "Characteristic and Applications of Rectangular Microstrip Antennas", SAND75-0339, July 1975.

2. G. H. Schnetzer, "Rectangular Microstrip Design Handbook", Sandia Internal Memorandum, Feburary 1977.

3. Ramo S. and Whinnery J. R., "Fields and Waves in Modern Radio", John Wilen & Sons, 1953, pp 356-358.

4. Jasik, "Antenna Engineering Handbook", McGraw Hill, 1961, pp 2-46 to 2-50.

5. Ramo S. and Whinnery J. R., "Fields and Waves in Modern Radio", John Wiley & Sons, 1953, pp 321-334.

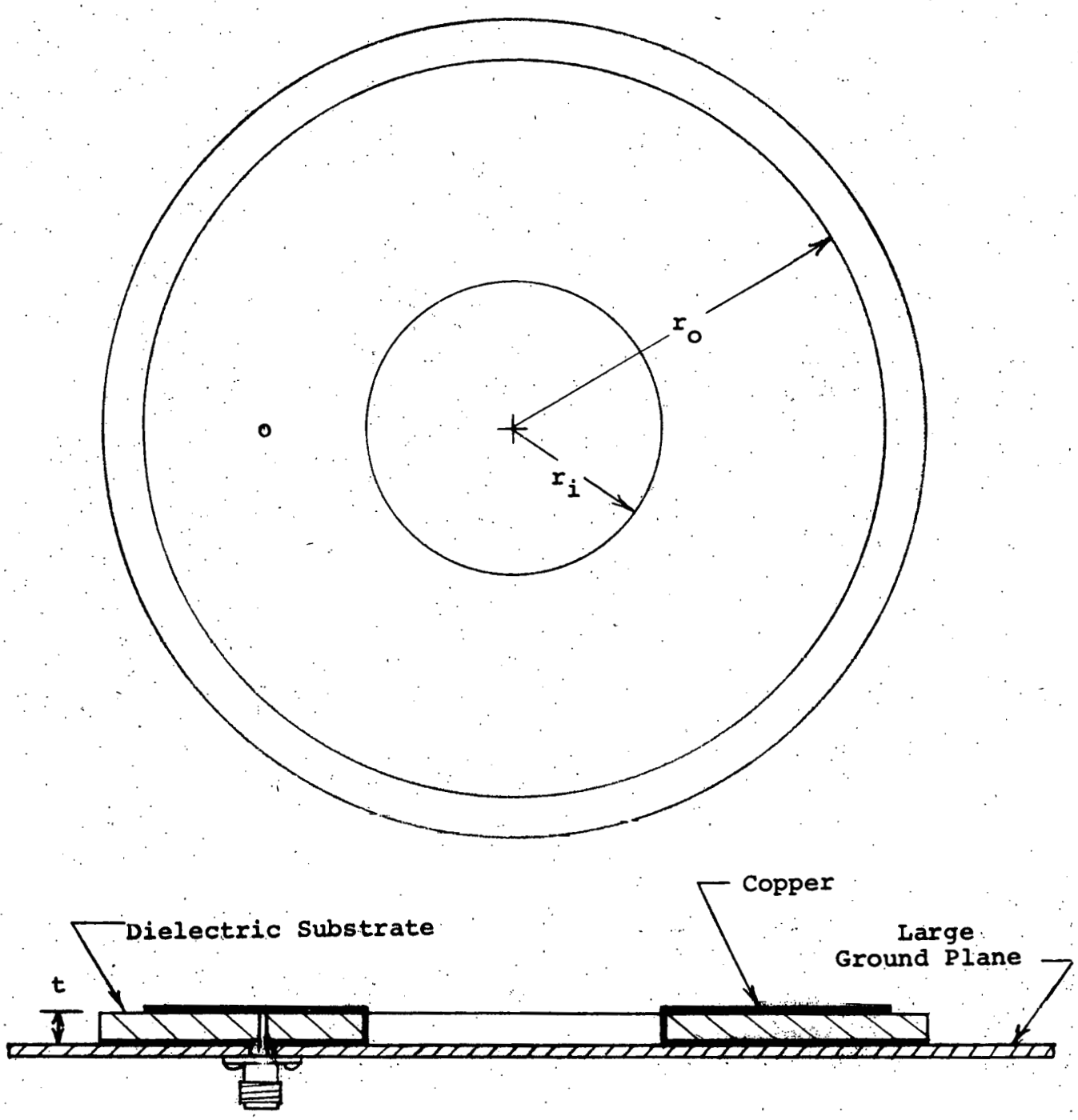

Fig. 1. Circular Microstrip Antenna

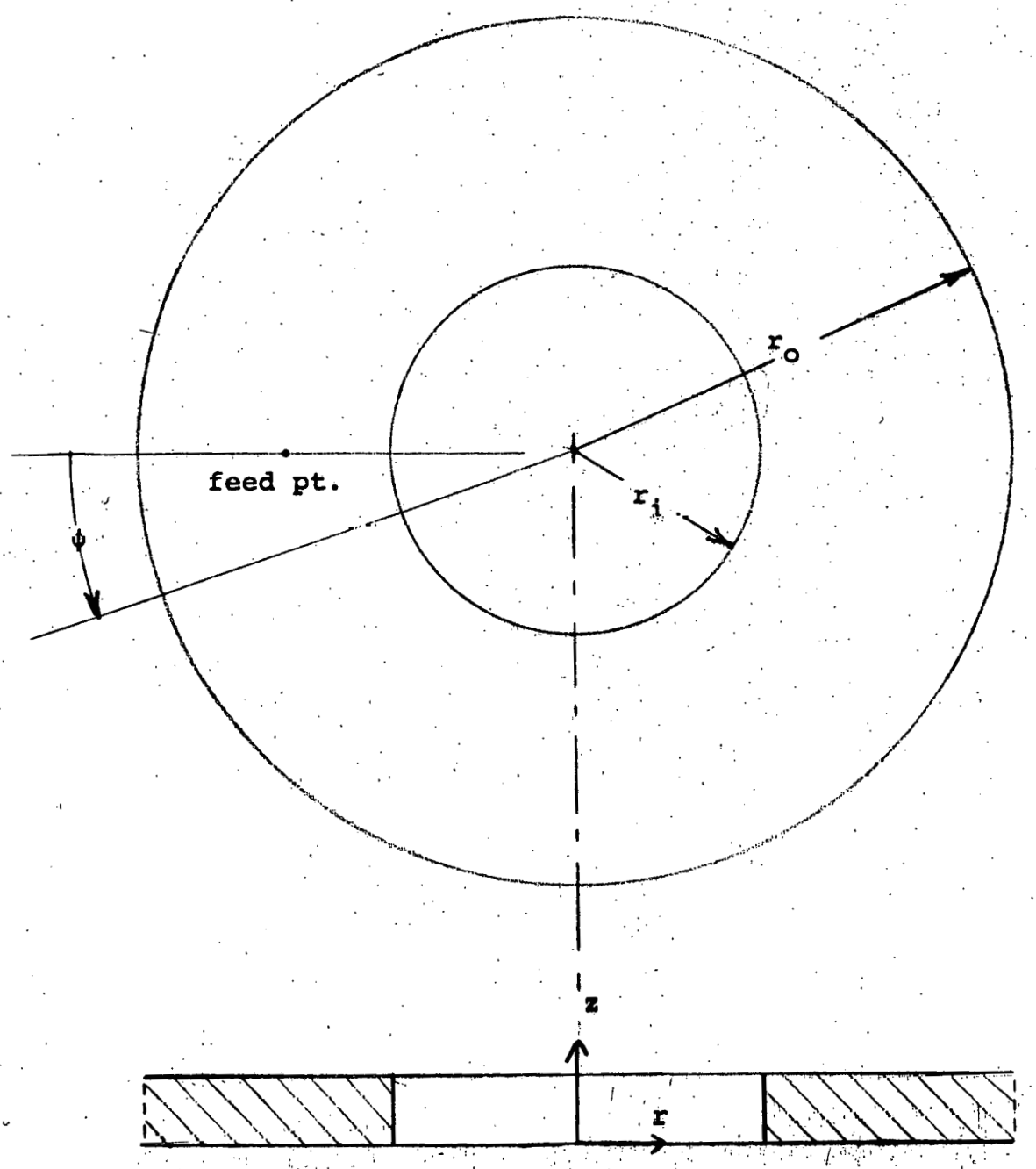

Fig. 2. Coordinate System for Analysis

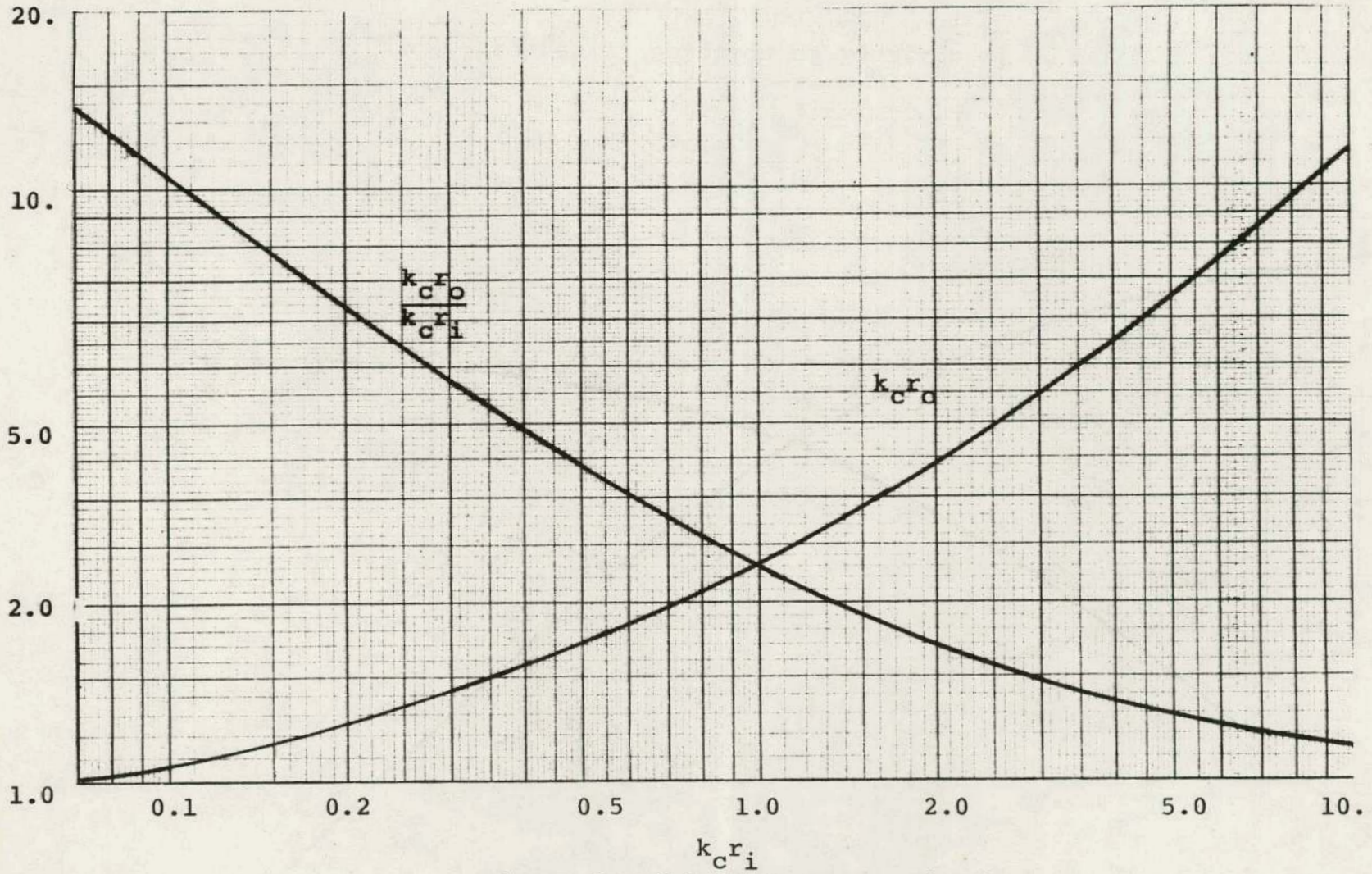

Figure 3. Solution of Equation 9
Zero Order Mode

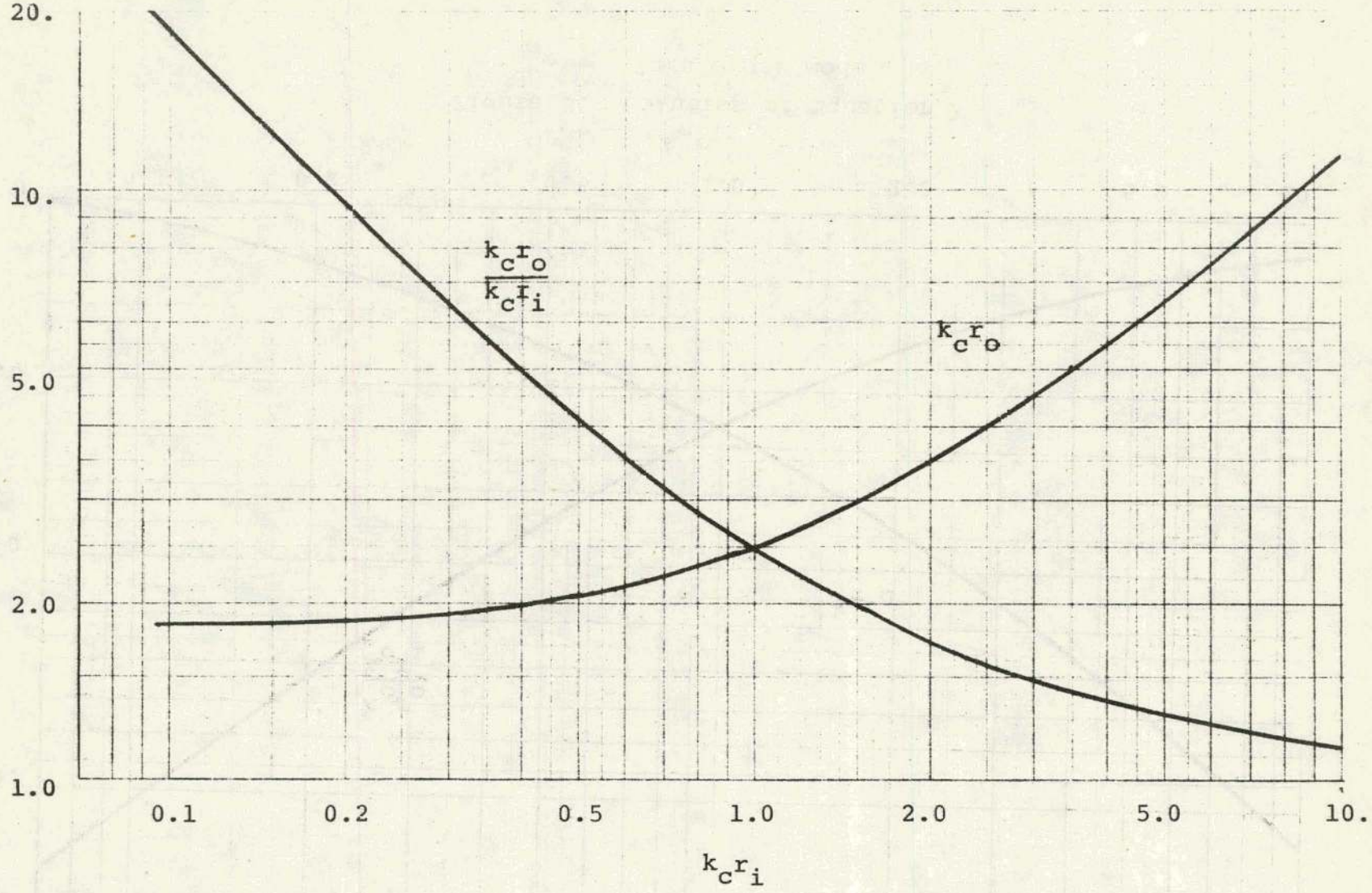

Figure 4. Solution of Equation 13
1st Order Mode

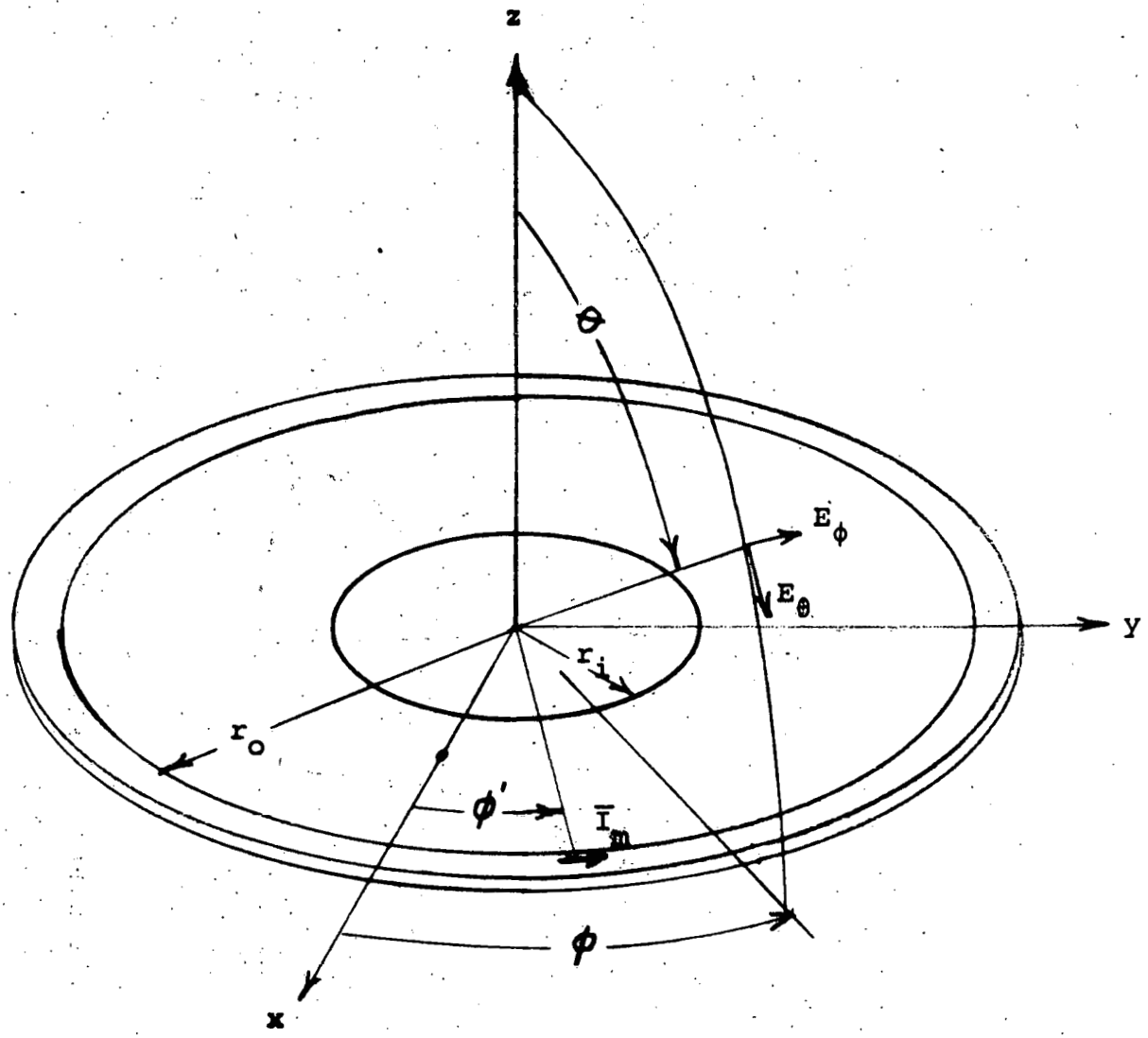

Figure 5. Antenna Pattern Coordinate System

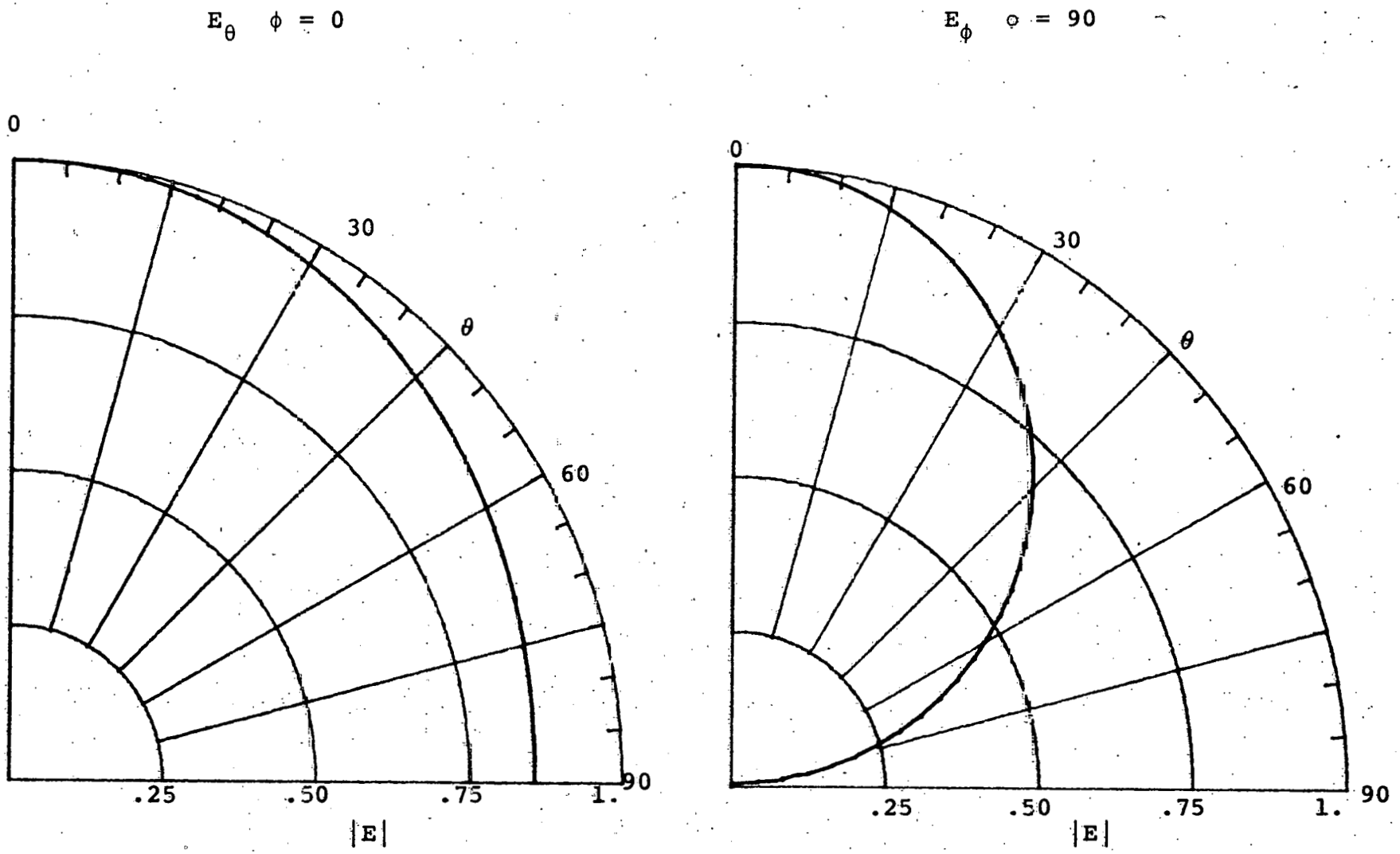

Figure 6. Circular Microstrip Antenna
(r_o/λ = 0.1, ν = 1)

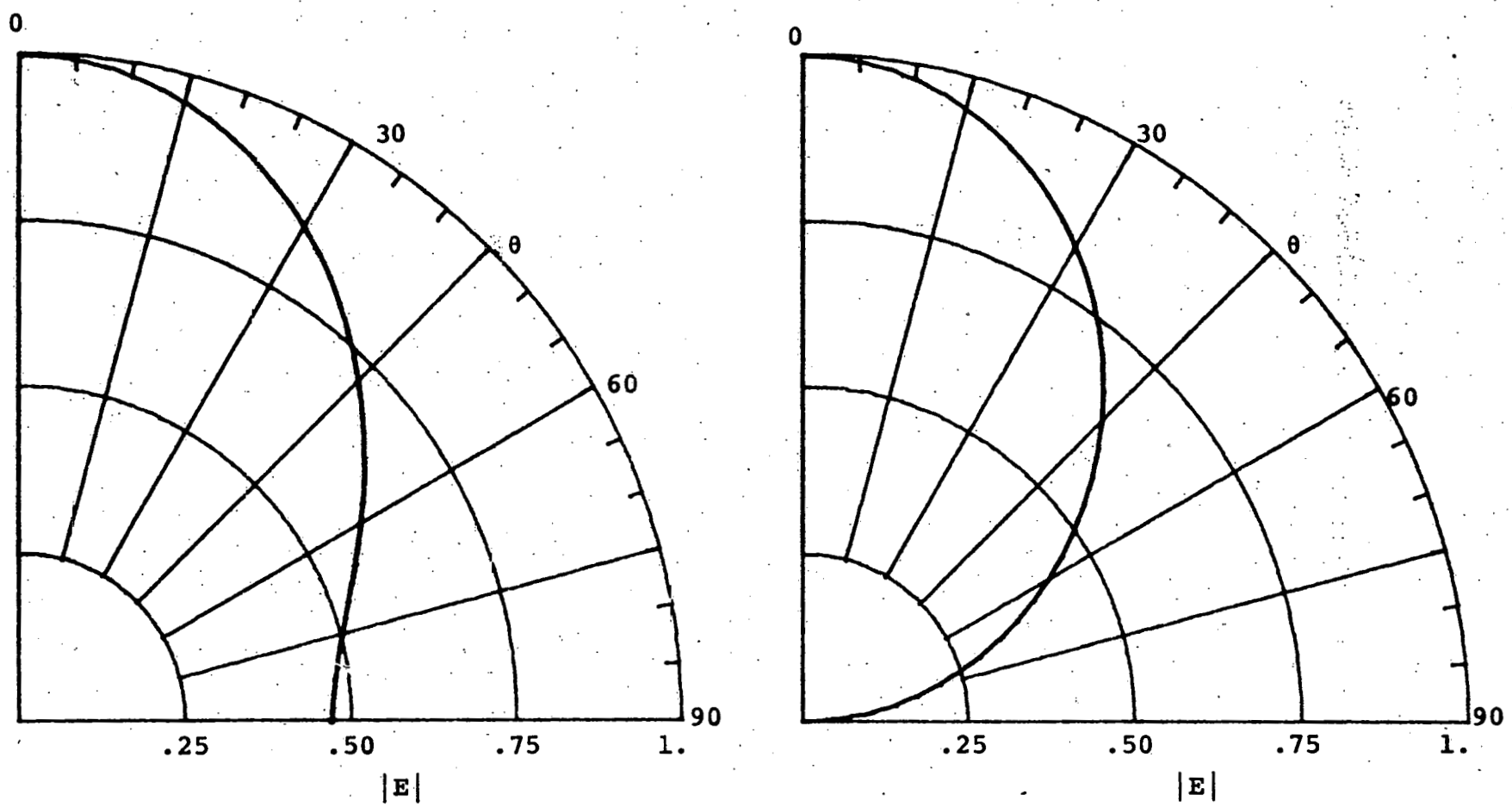

Figure 7. Circular Microstrip Antenna
($r_o/\lambda = 0.2$, $\nu = 1$)

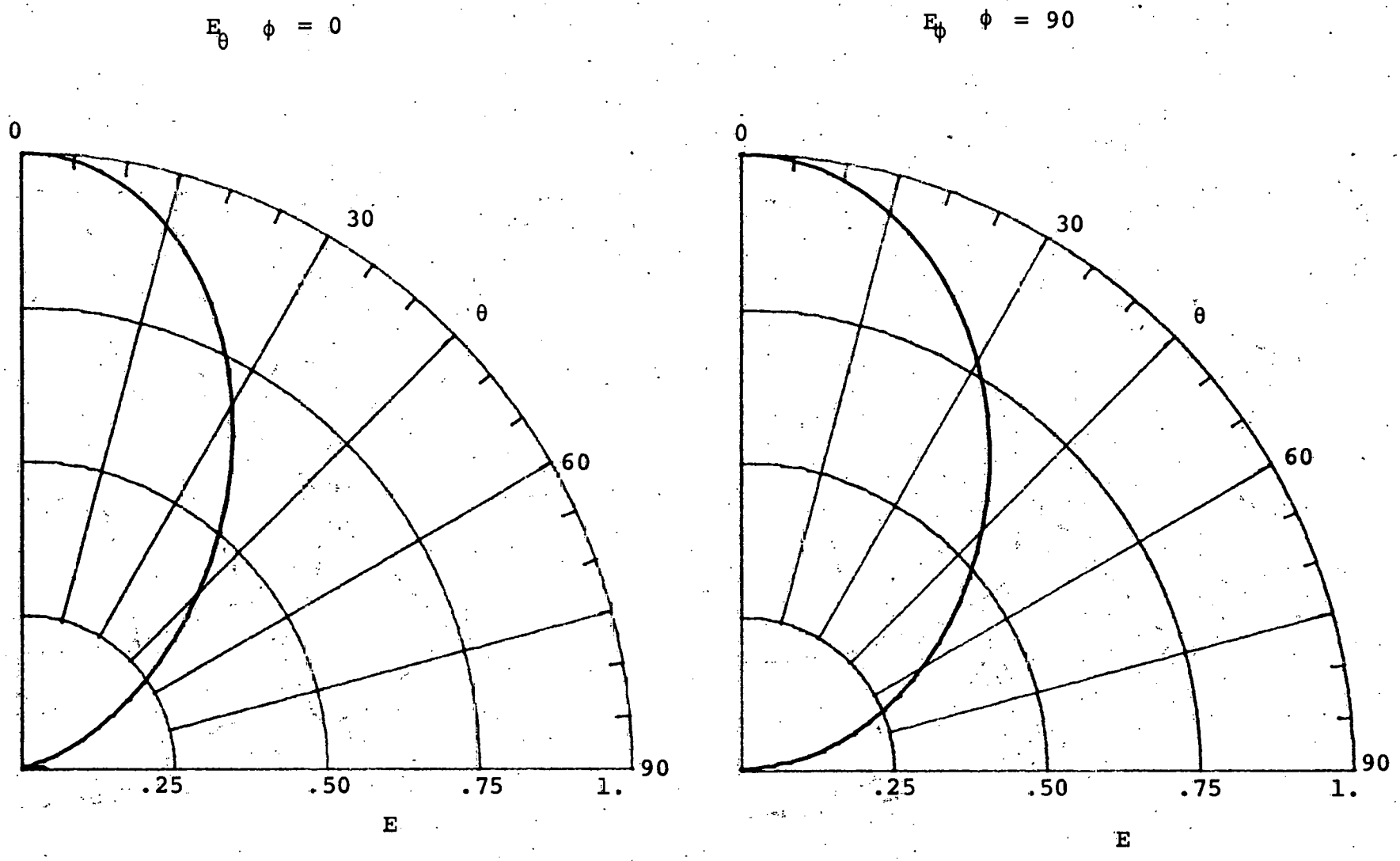

Figure 8. Circular Microstrip Antenna
(r_o/λ = 0.3, ν = 1)

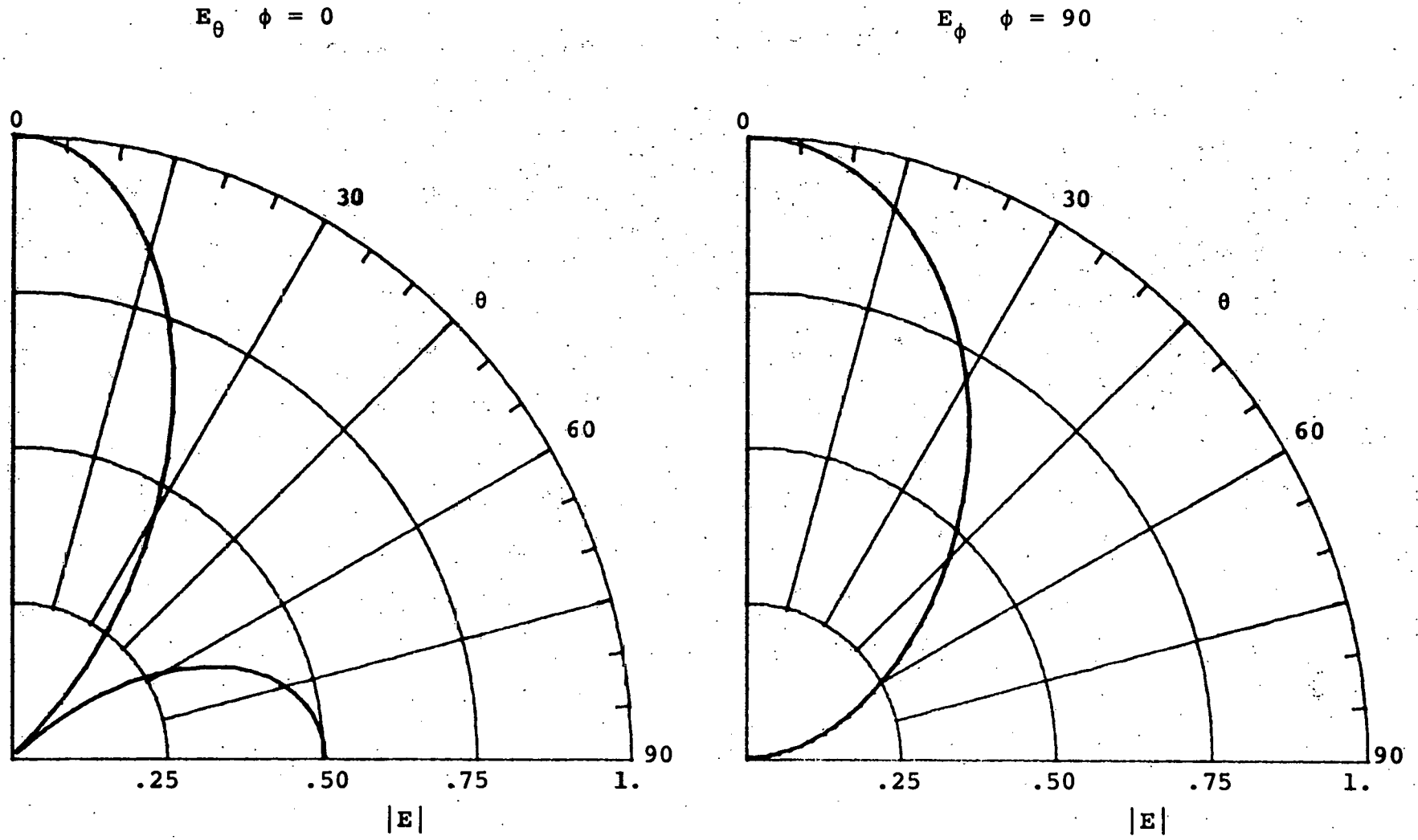

Figure 9. Circular Microstrip Antenna
($r_o/\lambda = 0.4$, $\nu = 1$)

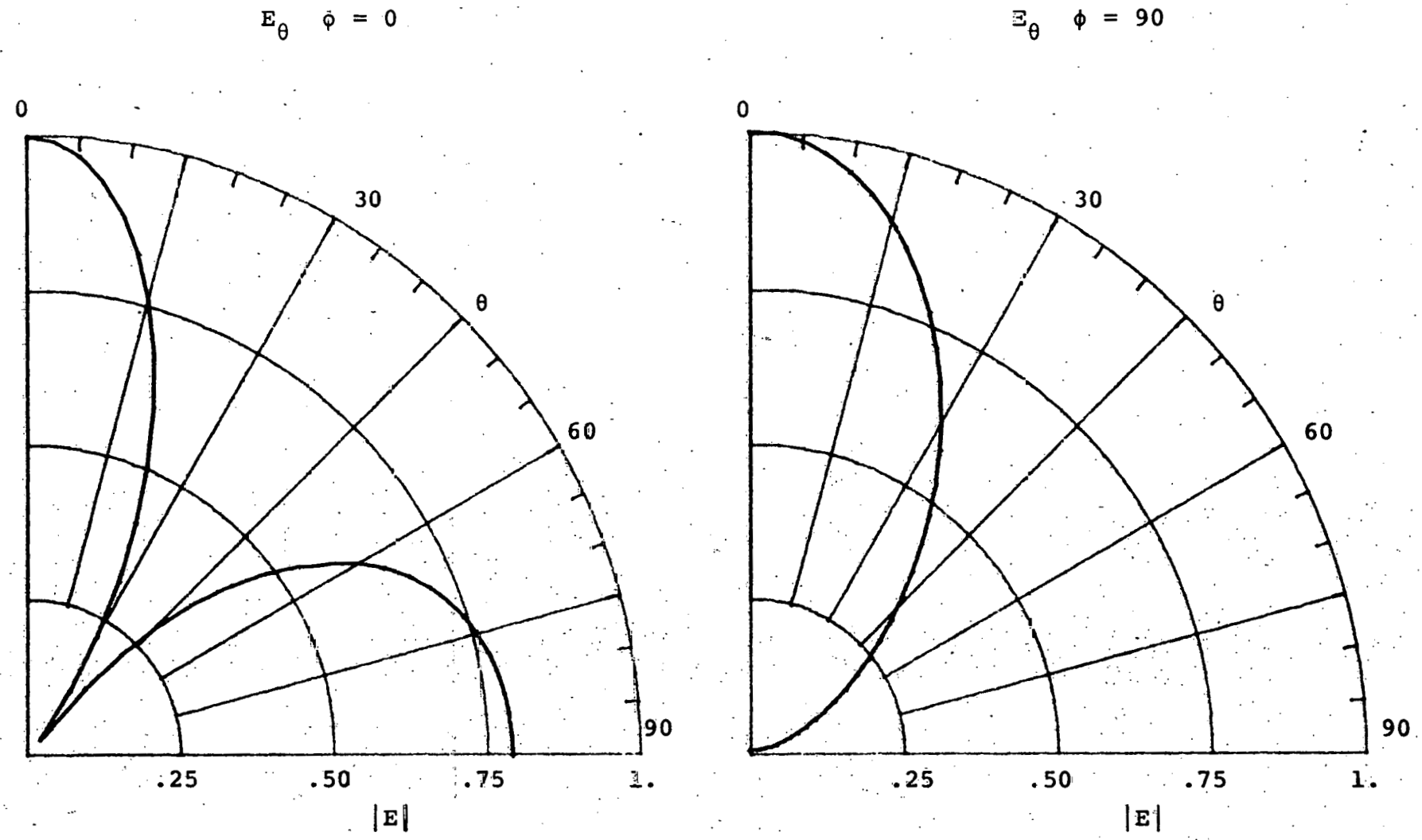

Figure 10. Circular Microstrip Antenna
(r_o/λ = 0.5, ν = 1)

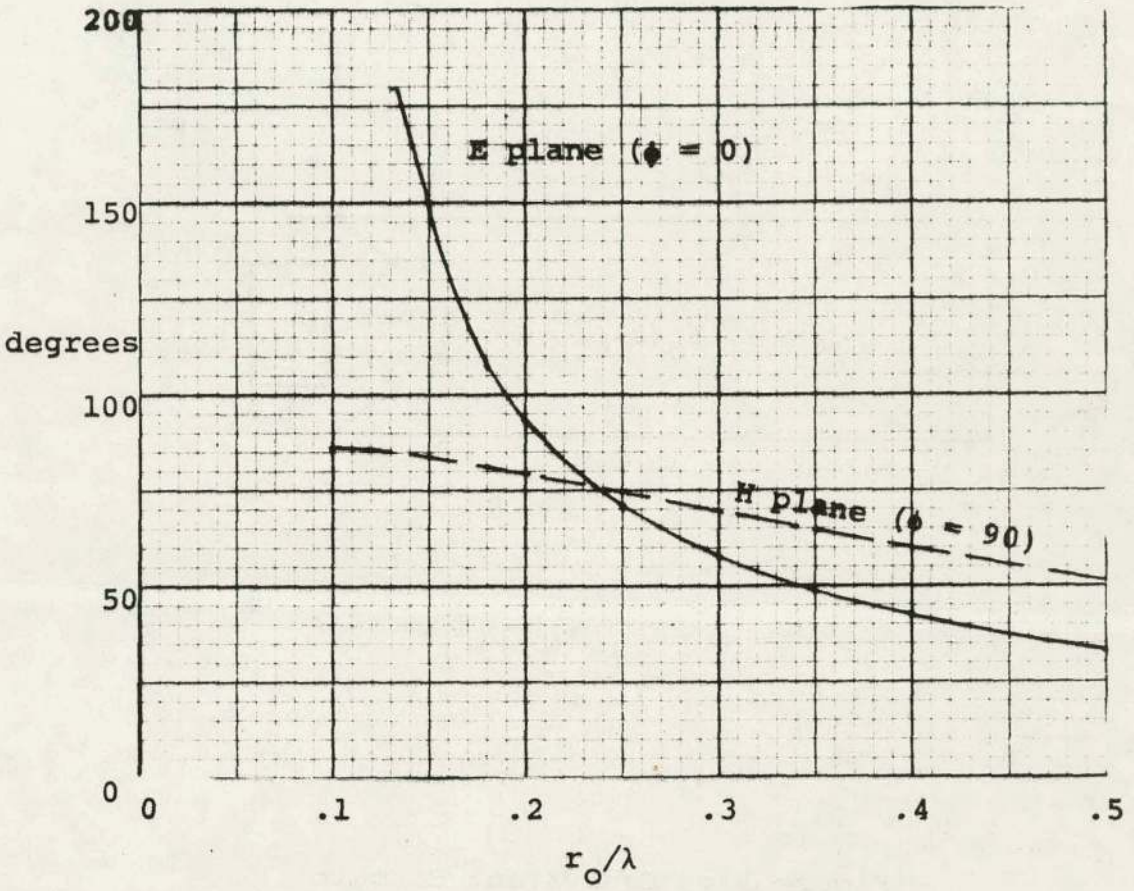

Figure 11. Circular Microstrip Antennas
Half Power Beamwidths

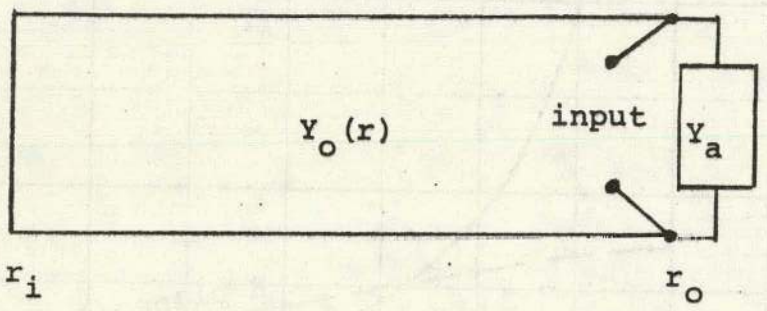

Figure 12. Equivalent Circuit

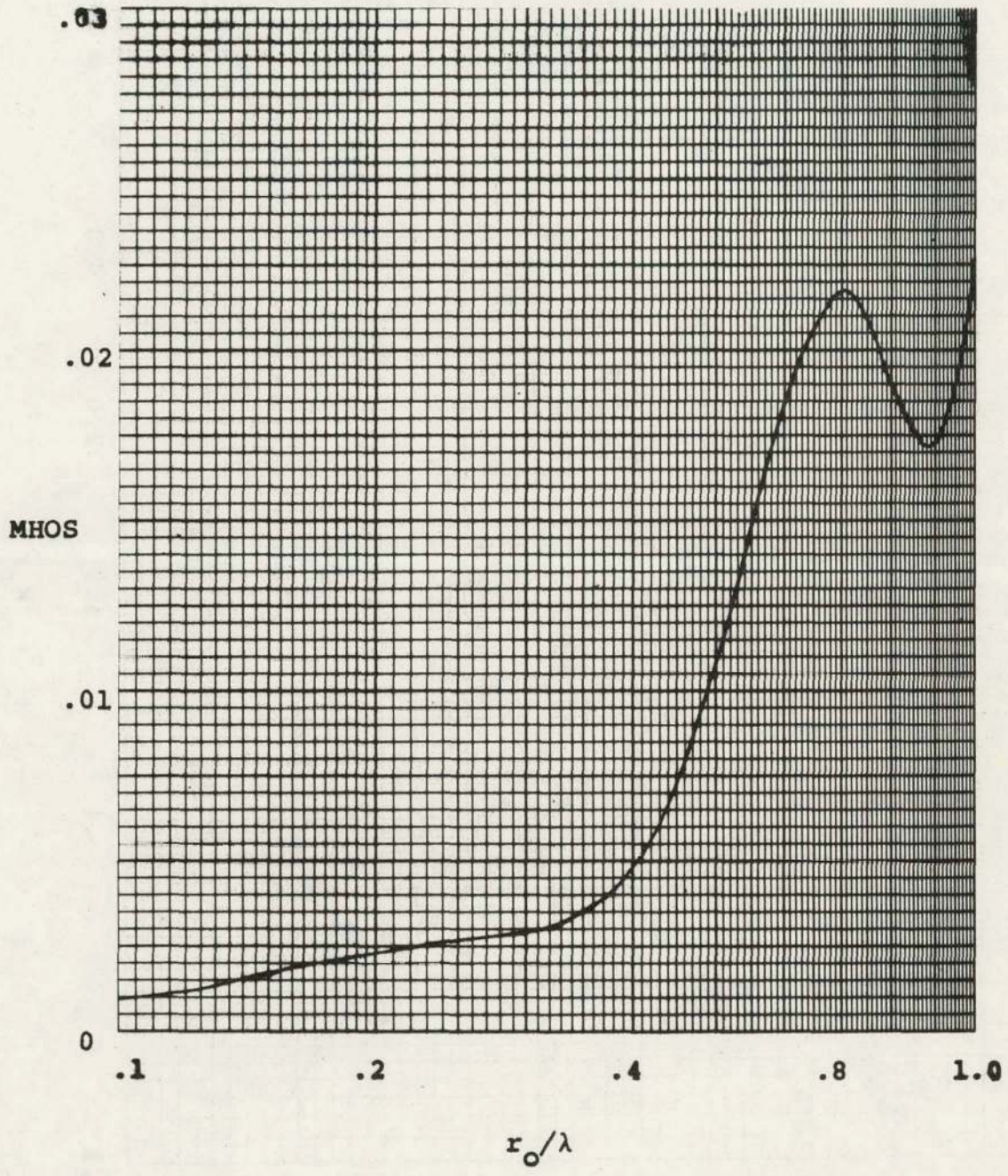

Figure 13. Radiation Conductance

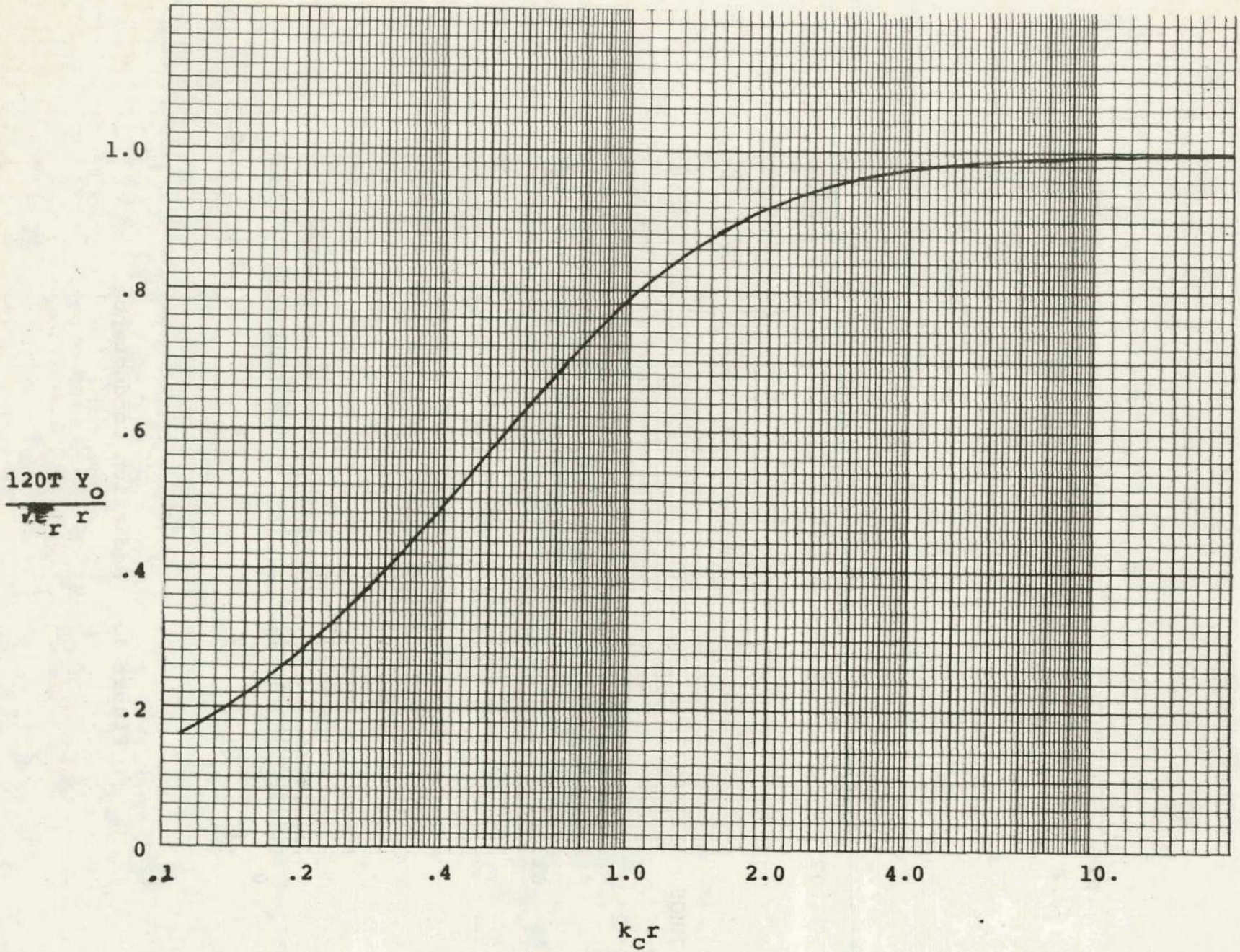

Figure 14. Normalized Characteristic Admittance

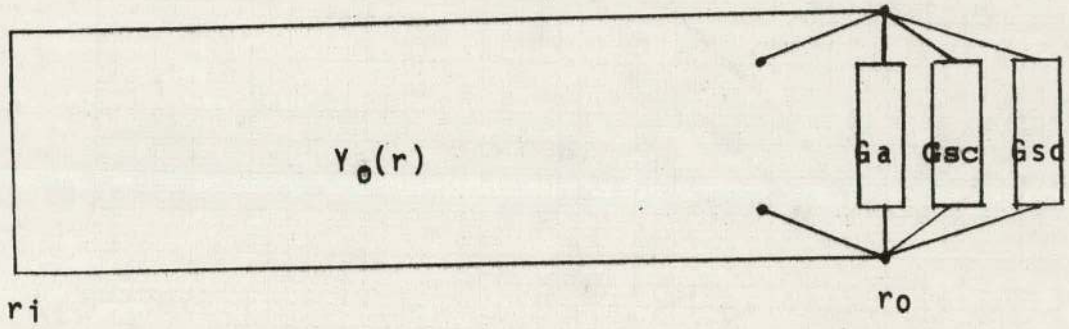

Figure 15. Equivalent Circuit with Losses

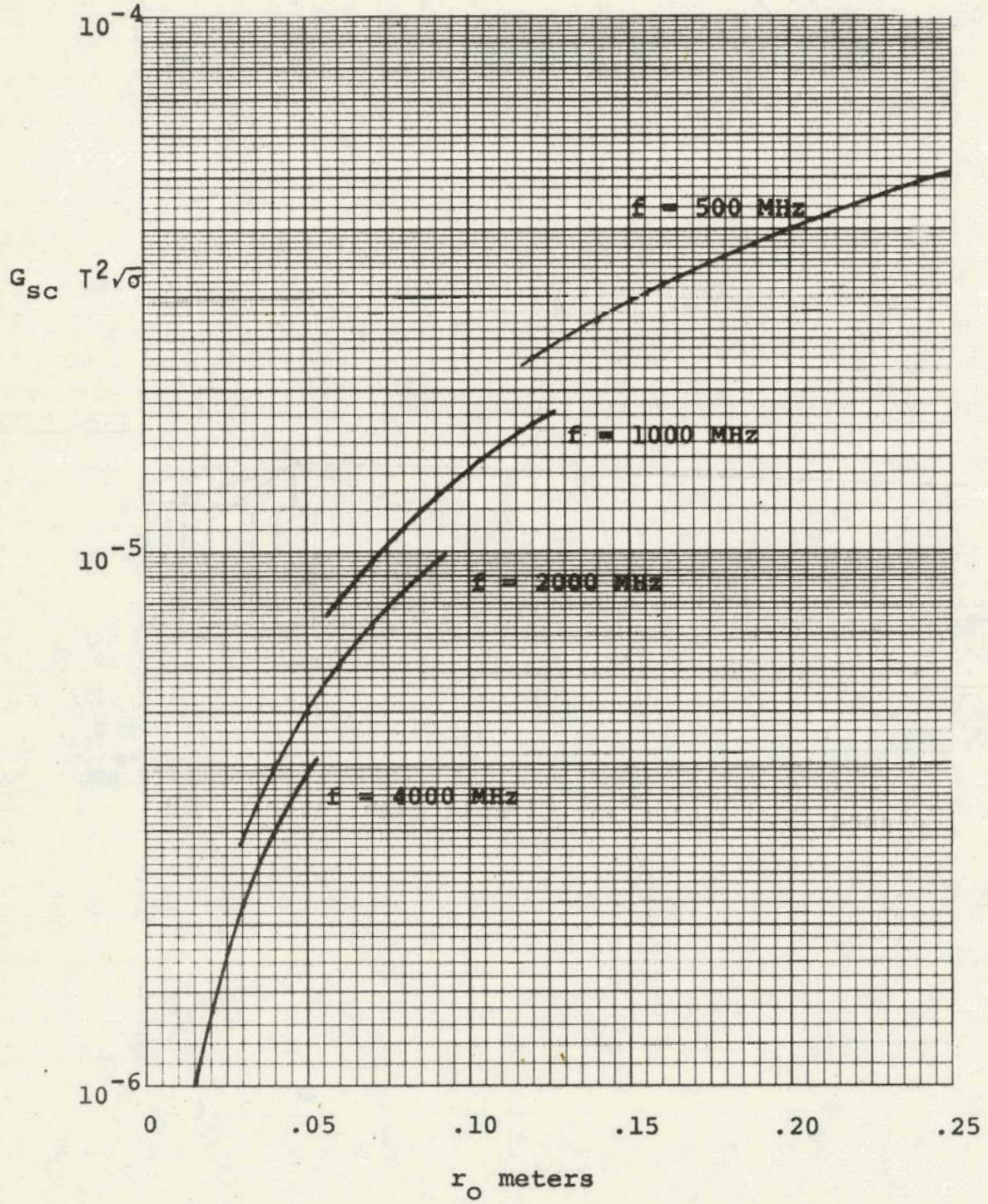

Figure 16. Conductor Loss Factor $\varepsilon_r = 2.5$

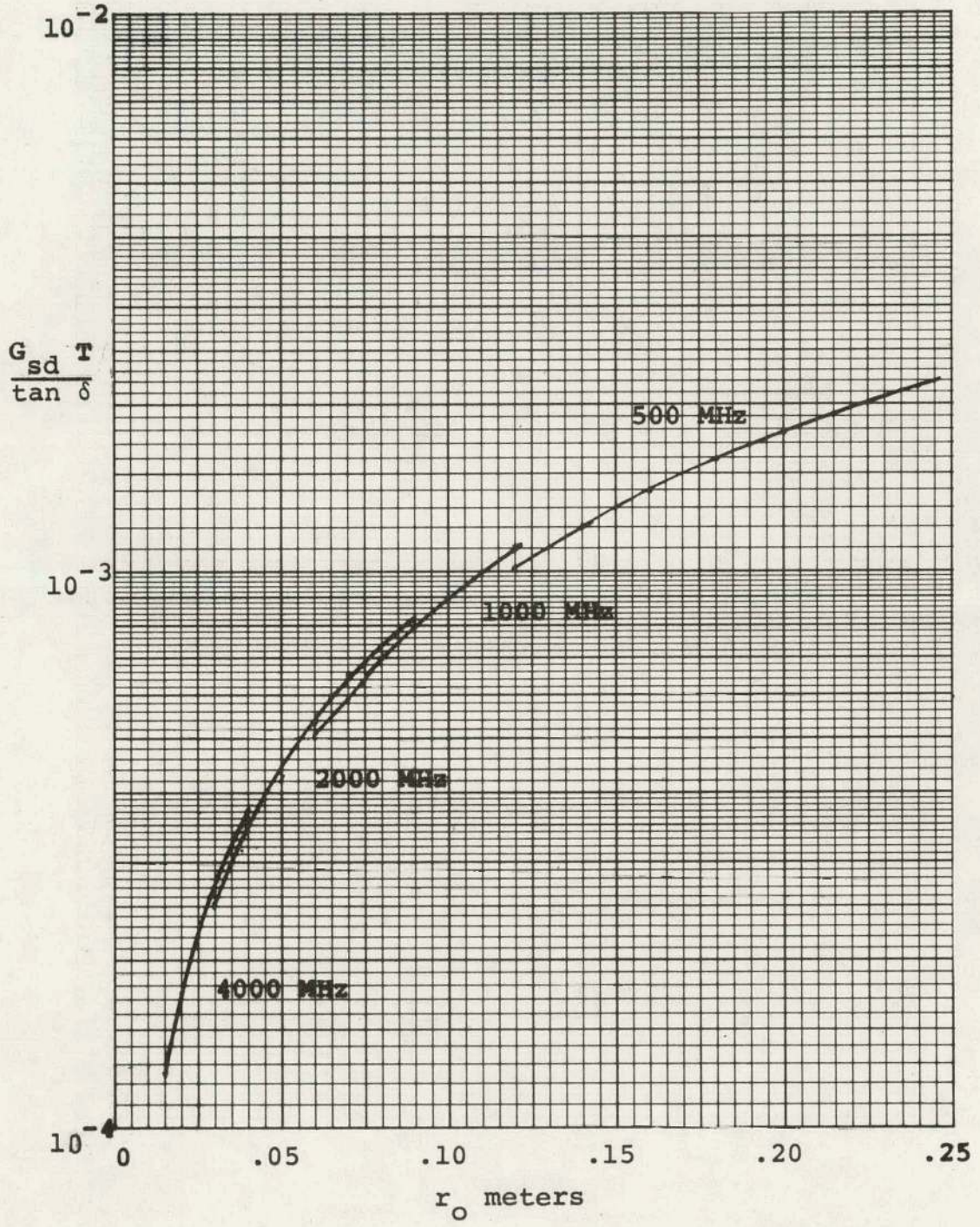

Figure 17. Dielectric Loss Factor $\varepsilon_r = 2.5$

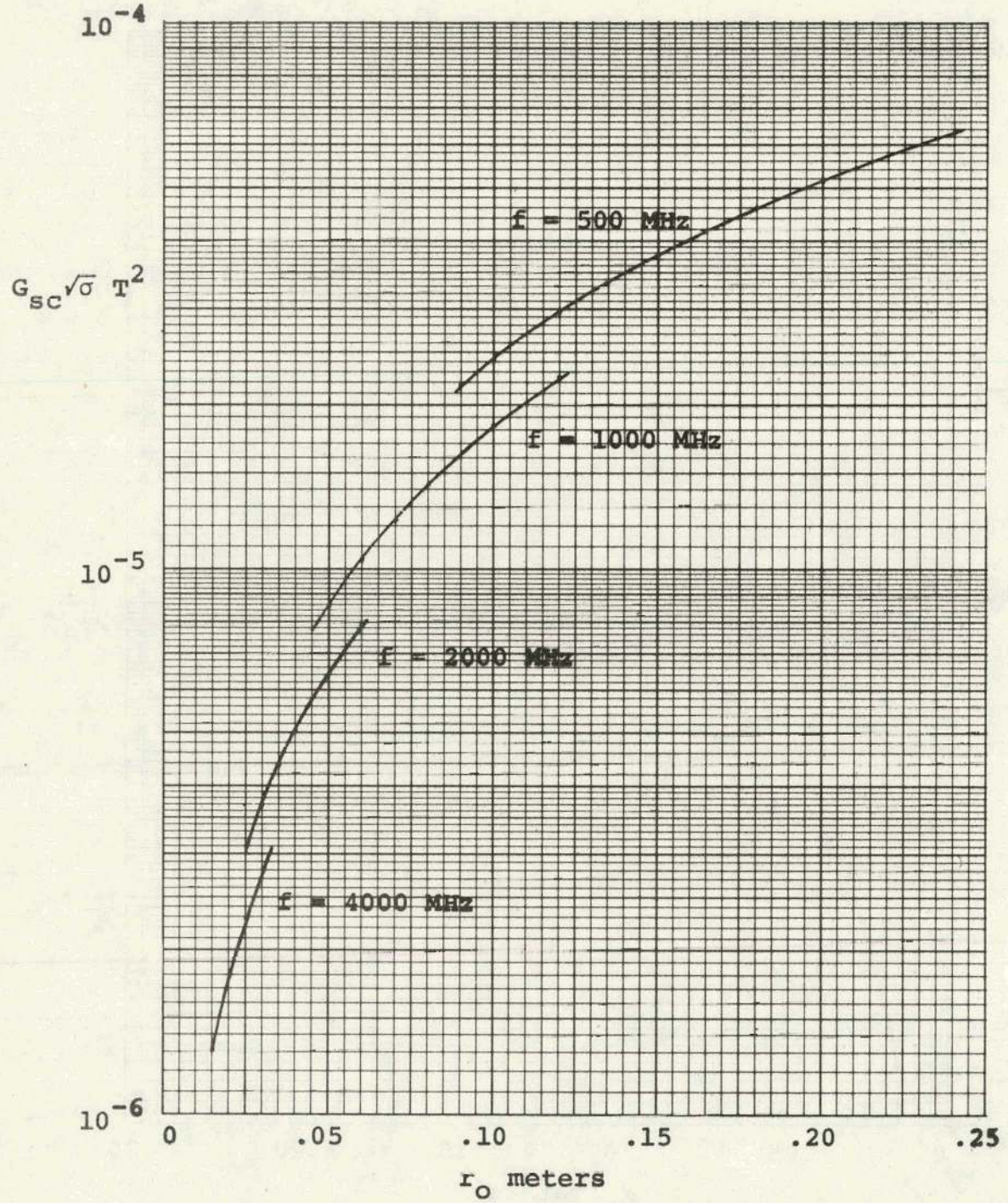

Figure 18. Conductor Loss Factor $\varepsilon_r = 4.0$

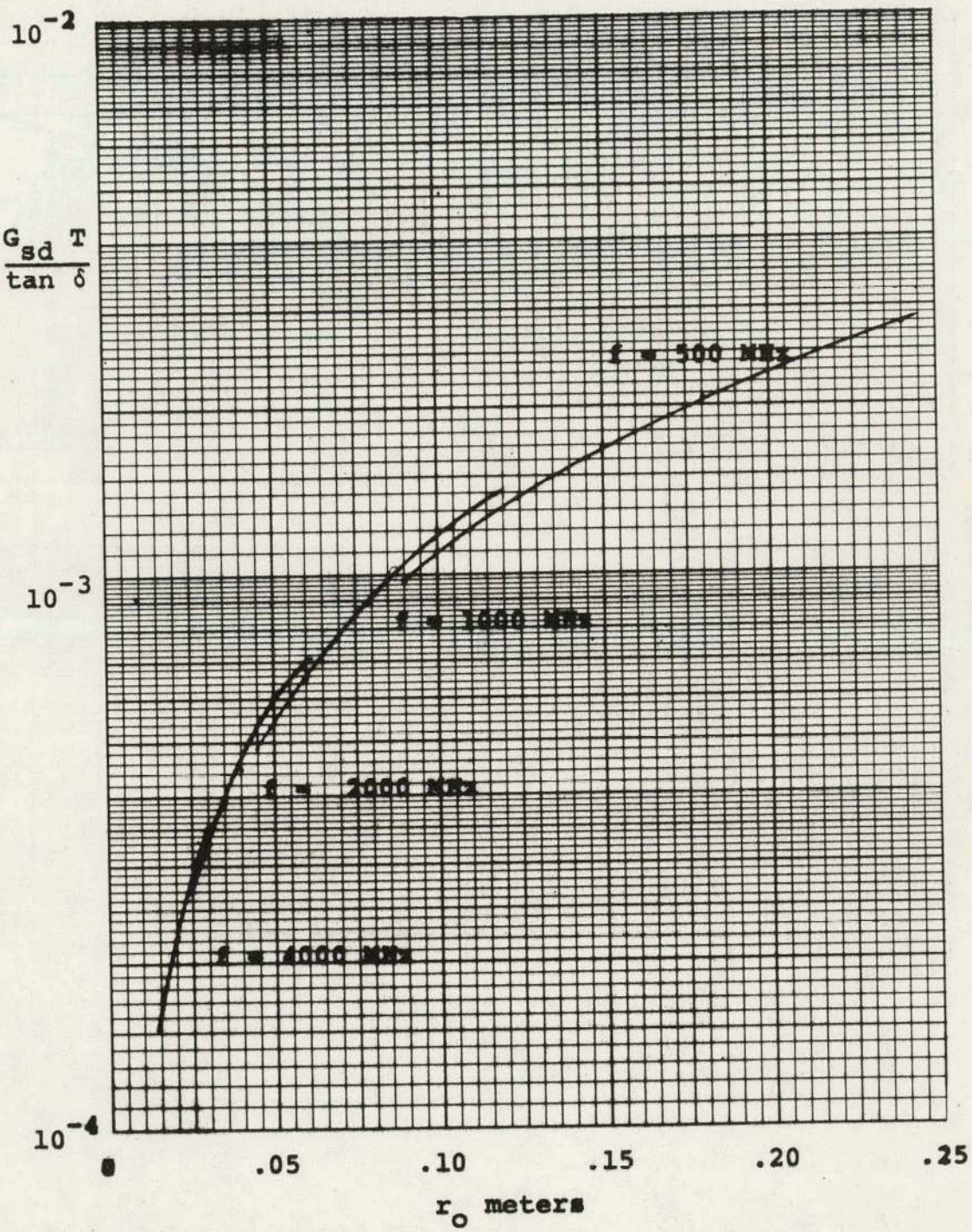

Figure 19. Dielectric Loss Factor $\varepsilon_r = 4.0$

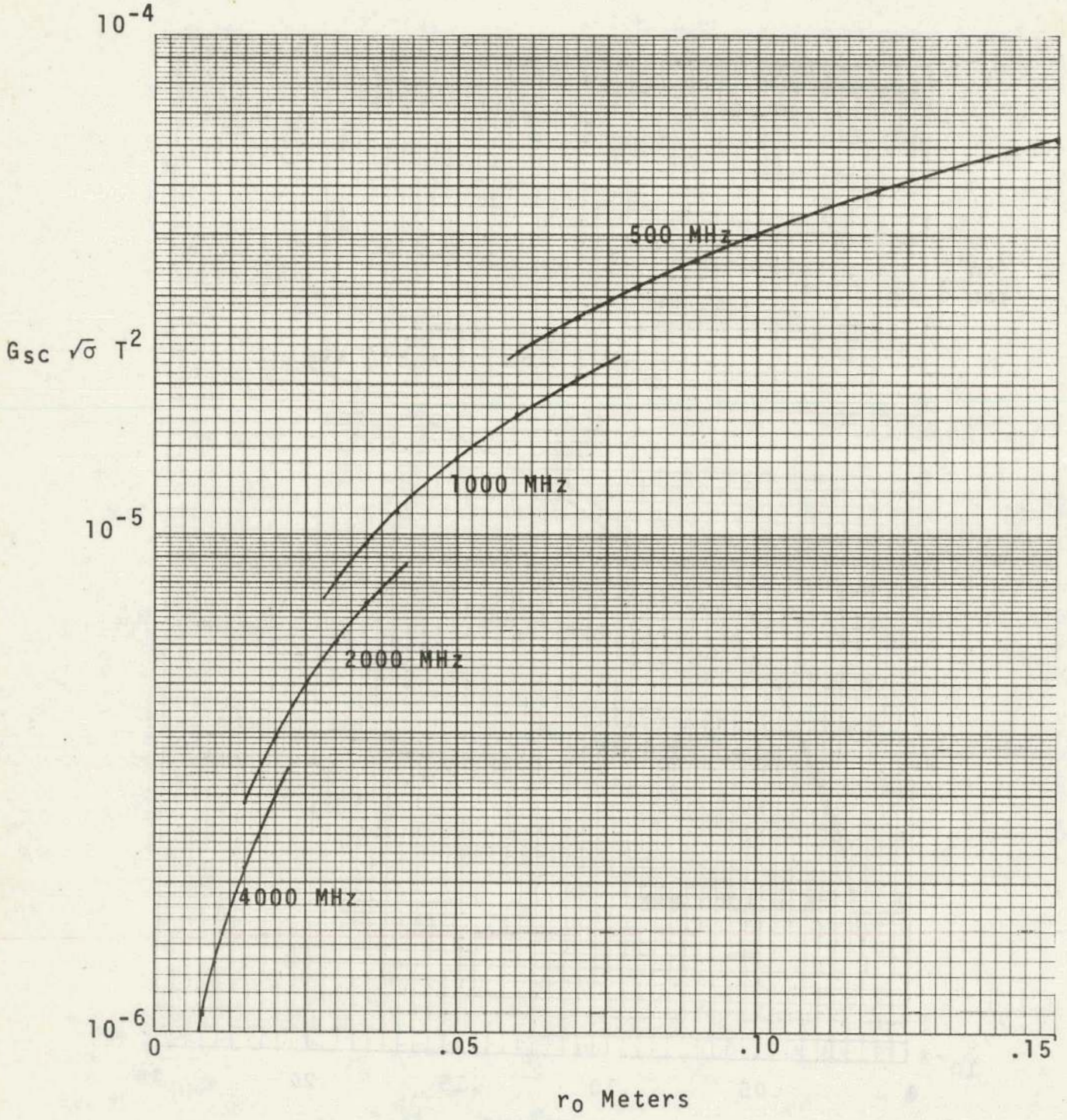

Figure 20. Conductor Loss Factor $\varepsilon_r = 10.0$

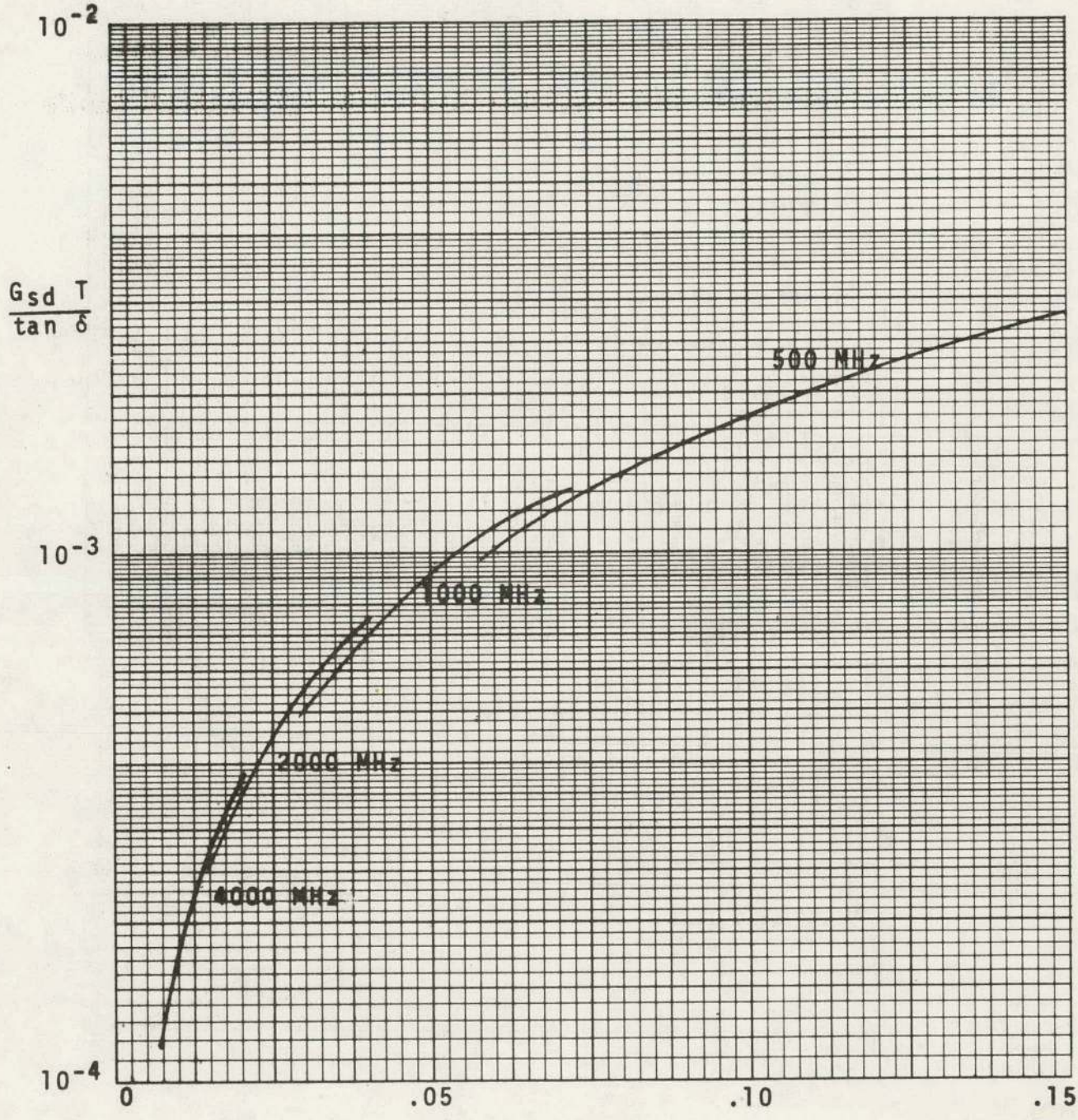

Figure 21. Dielectric Loss Factor $\varepsilon_r = 10.0$

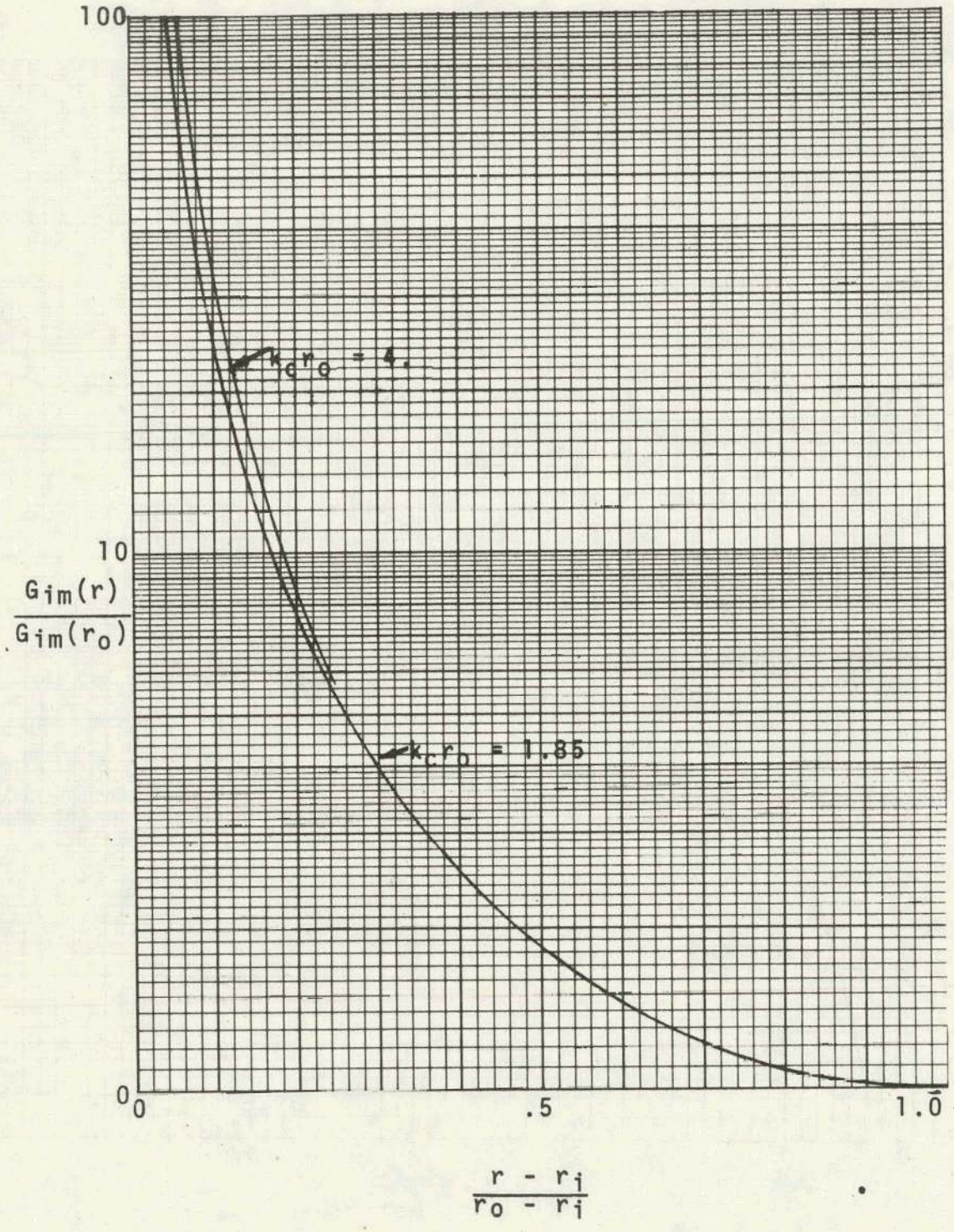

Figure 22. Ratio of Feed Point Conductance to Aperture Conductance

DISTRIBUTION

2120 G. W. Rodgers
2123 P. J. Komen
2123 P. A. Gelt
2123 R. D. Bentz
2123 R. C. Buehler
2123 R. A. Leighninger
2123 G. H. Schnetzer (6)
2125 R. J. Chaffin
2125 W. H. Schaedla
3141 L. S. Ostrander (5)
3151 W. L. Garner (3)
8266 E. A. Aas (2)
3171 R. P. Campbell
for ERDA/TIC (25)